Available online at www.sciencedirect.com
SCIENCE DIRECT®
International Journal of Pharmaceutics 278 (2004) 239–254
international journal of pharmaceutics
www.elsevier.com/locate/ijpharm

Incorporation of hydrophobic porphyrins into liposomes: characterization and structural requirements

F. Postigo [a], M. Mora [a], M.A. De Madariaga [a], S. Nonell [b], M.L. Sagristá [a,*]

[a] *Departament de Bioquímica i Biologia Molecular, Facultat de Química, Universitat de Barcelona, Martí i Franquès 1, Barcelona 08028, Spain*

[b] *Grup d'Enginyeria Molecular, Institut Químic de Sarriá, Universitat Ramon Llull, Via Augusta 390, Barcelona 08017, Spain*

Received 29 October 2003; received in revised form 20 February 2004; accepted 3 March 2004

Available online 14 May 2004

Abstract

The ability of photosensitisers to give reactive oxygenated products is considered decisive for photodynamic applications, but the hydrophobic nature of many porphyrins makes necessary to obtain suitable pharmaceutical formulations. This paper reports the structural photosensitiser features that allow the preparation of stable liposomal formulations. Metallated and non-metallated TPPs and TPyPs and different lipid/porphyrin ratios were considered in order to procure liposomal preparations containing porphyrin concentrations adequate to necessary doses. The results show that the incorporation of porphyrins into liposomes can be related with their ability to form aggregates in a watery media. Thus, ZnTPP, which structural properties avoid the formation of aggregates, was efficiently incorporated into stable liposomes. Moreover, the efficient generation of singlet oxygen by ZnTPP liposomal suspensions has been shown. Because of this, the synthesis of hydrophobic porphyrin derived structures or other sensitisers, which do not aggregate in a watery media and with Q-bands shifted to higher λ values than ZnTPP, will be efficiently incorporated into liposomes and useful for clinical applications.

Keywords: Liposomes; Porphyrins; Characterization; Interaction; Singlet oxygen

1. Introduction

Metallated- and non metallated-macrocyclic compounds, including porphyrins, have been widely studied as photosensitsers of living organisms in light-induced reactions (Henderson and Dougherty, 1992; Bonnett, 1995; Ben-Hur et al., 1995; Müller-Breitkreutz et al., 1995; Ben-Hur and Horowitz, 1996; Reddi, 1997). Furthermore, some of these products can be used in the detection of tumours by magnetic resonance imaging (MRI) (Brockhorst et al., 1994; Niesman et al., 1994; Berezin et al., 1997). The approval of Photofrin® has encouraged the accelerated development of second-generation photosensitisers. Photofrin is a commercial preparation derived from hematoporphyrin, consisting of a mixture of 60 hematoporphyrin esters and ethers containing monomers, dimers and oligomers in the proportion 22:23:55. It was the first drug to be granted approval for cancer photodynamic therapy (in Canada, 1993) and is currently the main drug in use around the world in this field (Bonnett, 2000). The effectiveness of these products can be affected by the quantum efficiency of the photosensitiser in situ

* Corresponding author. Tel.: +34-93-4021212; fax: +34-93-4021219.
E-mail address: sagrista@bq.ub.es (M.L. Sagristá).

0378-5173/$ – see front matter © 2004 Elsevier B.V. All rights reserved.
doi:10.1016/j.ijpharm.2004.03.004

or by their localisation at the time of activation with light.

Photosensitisers are usually aromatic molecules which are efficient in the formation of very toxic short-lived species after the irradiation with visible or near visible light in the presence of oxygen. Following the absorption of light the photosensitiser is promoted from its ground state into an electronically excited triplet state via a short-lived excited singlet state. The excited triplet can produce oxygenated products (mechanism reaction type I) or to form singlet oxygen, $^1O_2$ (mechanism reaction type II). The extent of type I and II reactions depends on the photosensitiser, the substrate, the oxygen concentration, and the binding of the photosensitiser to the substrate, although it has been reported that singlet oxygen is the major damaging specie produced (Henderson and Dougherty, 1992; Bonnett, 1995). The presence of these highly reactive species in a cellular environment makes possible the degeneration of biological structures, like membranes (Henderson and Dougherty, 1992; Bonnett, 1995). Thus, the first use of photosensitisers was directed to the destruction of malignant tumours, naming photodynamic therapy (PDT) the damage of living tissues by a combination of photosensitiser, visible light and oxygen (Henderson and Dougherty, 1992; Bonnett, 1995). On the other hand, photodynamic methods have also been considered for virus inactivation in blood samples before transfusion (North et al., 1993; Ben-Hur et al., 1995; Müller-Breitkreutz et al., 1995; Ben-Hur and Horowitz, 1996).

The first step towards PDT and MRI is the delivery of the porphyrins to the target tissue (Henderson and Dougherty, 1992). The transport of porphyrins in the bloodstream through liposomal vesicles has been shown to give a larger and more selective accumulation of the drug in neoplastic tissues (Schieweck et al., 1994; Segalla et al., 1994; Reddi, 1997; Berezin et al., 1997). Moreover, most of the porphyrins exert their photoactivity after preferential association with membranes, being the main targets of photodamage cellular components such as lipids and proteins (Hoebeke, 1995; Richelli, 1995). In this way, liposomes can make easy the transfer of very lipophilic porphyrins from the delivery system to cellular membranes.

Liposomes can be used to enhance the clinical effects of photosensitisers, to reduce their toxicity and to protect them from metabolism and immune responses (Oku, 1991; Oku et al., 1992; Hoebeke, 1995; Reddi, 1997). Liposomes with specific characteristics can be elaborated in order to achieve a better target-directed drug delivery. Target-sensitive liposomes, composed of lipids forming a membrane that is intrinsically unstable, can be stabilised by anchoring a specific antibody in the membrane through covalent attachment. When antibody-coated liposomes were specifically bound to antigen-presenting target cells the ability of the antibody to stabilise the membrane is reduced and liposomes disintegrate releasing their content. Temperature-sensitive liposomes, undergoing phase transition at a specific temperature, are perturbed and break down when they pass through the warmed-target releasing their content. pH-sensitive liposomes, which membrane is stabilised by addition of materials that are charged at neutral pH but lose their charge at low pH, can fuse with biomembranes and/or destabilise at low pH. Incorporation of polyethylenglycol or monosialoganglioside in liposomal membranes can change the fate of injected liposomes by preventing liposomal uptake by macrophages. Thus, liposomes with a hydrophilic cover have a prolonged blood stream circulation time. After the selective accumulation of the photosensitiser, the local irradiation of neoplastic tissues with the appropriate light will make possible the destruction of the tumour.

The photophysical properties of porphyrins strongly depend on their aggregation state (Ricchelli, 1995; Abós et al., 1997; Ricchelli et al., 1998). Porphyrin monomers exhibit the well-known visible spectrum consisting in an intense Soret band (λ_{max} = 390–415 nm, $\varepsilon = 1 \times 10^5$ to $2 \times 10^5\ M^{-1}\ cm^{-1}$) and four weaker bands (called Q-bands) in the 450–700 nm range. Porphyrin monomers show a significant fluorescence emission, with two bands (620–640 and 660–690 nm) and fluorescence lifetimes (τ) in the 10–18 ns range (Ricchelli et al., 1998). These properties drastically change upon aggregation; for large self-associated suprastructures, the porphyrin absorption coefficient decreases drastically, the Soret band is shifted and the fluorescence yields and lifetimes become very low. The aggregation, moreover, reduces the yield and the lifetime of the porphyrin triplet state, thus reducing the $^1O_2$ formation yield (Boyle and Dolphin, 1996; Ricchelli et al., 1998). In this way, the literature describes two modes of porphyrin aggregation: a face-to-face aggregation (H-aggregates)

(Hunter and Sanders, 1990; Ribó et al., 1994) and an edge-to-edge interaction (J-aggregates) (Ribó et al., 1994; Akins et al., 1996; Micali et al., 2000), but only monomeric species and possible planar aggregates, observed in liposomal and mitochondrial membranes, are endowed with significant photosensitising ability (Ricchelli, 1995; Ricchelli et al., 1998).

The singlet-oxygen-mediated photodamage will increase when the porphyrins and targets are located in hydrophobic regions (Sandberg and Romslo, 1981; Ricchelli, 1995), since the lifetime of $^1O_2$ in hydrocarbon solvents or micelles (20–25 μs) is significantly higher than the corresponding in water (3–4 μs). Moreover, the maximal efficiency of the photodynamic process is obtained when the dye becomes closely associated with the target due to the short diffusion path of cytotoxic species, including singlet oxygen, during their lifetimes (less than 0.1 μm in biological material) (Moan, 1990; Ricchelli, 1995). These facts together with the water-insoluble nature of several photoactive porphyrins, which require a lipid-based delivery system for their systemic injection, lead us to study the requirements of hydrophobic porphyrins for incorporation into liposomes with high efficiency. Moreover, we will try to relate the porphyrin-liposomes incorporation efficiency to their structure and tendency to form aggregates in the liposomal system, and whether the incorporation of the photosensitiser into liposomes affects their ability to generate oxygen singlet.

2. Materials and methods

2.1. Materials

Imidazole, 5,10,15,20-tetraphenyl-21*H*,23*H*-porphine (TPP), 5,10,15,20-tetraphenyl-21*H*,23*H*-porphine zinc (ZnTPP), 5,10,15,20-tetraphenyl-21*H*,23*H*-porphine manganese (III) chloride (MnTPP), 5,10,15,20-tetra(4-pyridyl)-21*H*,23*H*-porphine (TPyP) were from Sigma-Aldrich Chemical Co. (St. Louis, MO, USA). *meso*-5,10,15,20-Tetrakis-(4-sulfonatophenyl-21*H*,23*H*-porphine (TPPS) and uroporphyrin I dihydrochloride (UP) were purchassed from Porphyrin Products (Logan, UT, USA). 5,10,15,20-Tetra(4-pyridyl)-21*H*,23*H*-porphine zinc (ZnTPyP) was obtained by metallation of TPyP at the Department of Organic Chemistry (A. Vallés, unpublished data). All the porphyrins used were pure with a minimal grade of 99%. C_{60} buckminsterfullerene was from Texas Fullerene Corporation (Houston, TX, USA). Synthetic L-α-palmitoleoylphospathidylcholine (POPC), L-α-dipalmitoylphosphatidylcholine (DPPC), L-α-dimiristoylphospatidylcholine (DMPC) and L-α-dioleoylphosphatidylserine (OOPS) are from Avanti Polar Lipids (Birmingham, AL, USA). All other chemicals were commercially available reagents of at least analytical grade. Milli-Q water (Millipore Bedford, Massachusetts system, resistivity of 18 MΩ cm) was used. Polycarbonate membranes are from Poretics Products (Livermore, CA, USA).

2.2. Preparation of liposomes

Intermediate unilamellar liposomes (IUV) for porphyrin incorporation were prepared either by extrusion or microemulsification following standard procedures. POPC or POPC/OOPS mixtures, alone or with the corresponding porphyrin, were solubilized in two milliliters of tetrahidrofuran (THF). To solubilize ZnTPyP the addition of two drops of methanol was necessary. The samples solubilized in THF were kept at 45 °C during one hour. Afterwards, the solvent was evaporated to dryness in a rotatory evaporator to deposit a lipid film on the walls of a test tube. In order to remove final traces of the solvent the films were kept in a vacuum desiccator for 12 h over $CaCl_2$. Multilamellar vesicles (MLVs) were prepared by hydration of the dried lipid films by vortexing for 30 min (alternating 30 s periods of heating and 30 s of vortexing) at a concentration of 10–20 mg lipid/ml of 50 mM imidazole–HCl buffer (pH 7.4). The MLVs dispersion was frozen and thawed (five times) and sonicated (bath sonicator, 60 min, 45 °C). To prepare IUVs by the extrusion methodology the MLVs dispersions were extruded twenty nine times sequentially through two stacked 0.8, 0.4 and 0.2 μm polycarbonate membrane filters using a LiposoFast-Basic extrusion device (Avestin, Ottawa, Canada). For microemulsification, the MLVs dispersions were introduced in an EmulsiFlex B3 device (Avestin, Ottawa, Canadá) and the fluid was pumped fifteen times at 200 kPa through the interaction chamber, where the suspension was separated into two streams that

collide with each other at high speed. During the extrusion or microemulsification processes the lipid suspensions were kept at 45 °C. TLC analysis showed that the lipids did not suffer degradation during the sonication process. The non-encapsulated porphyrin has been separated by centrifugation at 4000 rpm for 5 min. The absence of free porphyrin in the liposomal systems, after centrifugation at 4000 rpm, has been tested by Centricon YM-30 Filter Devices (Millipore, USA) and by gel filtration of the liposomal suspensions on Sephadex G-50 (Pharmacia Biotech, Uppsala, Sweden) columns. Free porphyrin was not detected in the filtrate of liposomal suspensions obtained by ultrafiltration, at 8000 rpm for 50 min, using the Centricon Filter Devices. In the same way, free porphyrin was not retained in Sephadex G-50 columns after the elution of the liposomal suspensions.

2.3. Porphyrin and lipid evaluation in liposomes

The porphyrin content in the liposomes was evaluated by measuring the absorption of each liposomal sample, free of non-entrapped porphyrin, at the λ_{max} of the Soret band of each phorphyrin, after liposomes disruption by the addition of THF. For liposomes disruption 24 volumes of THF were added to an aliquot of the liposomal suspension obtained in 50 mM imidazole–HCl buffer (pH 7.4) as indicated (THF/imidazole–HCl buffer, 24/1, v/v). The porphyrin concentration was determined by comparison with standard curves obtained in THF/imidazole–HCl buffer (24/1, v/v) using the appropriate porphyrin in the presence of the lipids at the corresponding molar ratios. The molar absorption coeficients (ε) and the λ_{max} of the Soret band for porphyrins in the absence and in the presence of lipids are indicated in Table 1.

Lipid concentration was quantified spectroscopically by phosphorus analysis ($\lambda = 820$ nm, $\varepsilon = 910\,cm^{-1}\,l\,g^{-1}$ of P_i) according to the method of Rouser et al. (1970).

2.4. Liposome characterization: vesicle size analysis and stability of the liposomal suspensions

Liposomes with incorporated porphyrins were characterised by the control of the particle size. The size and size distribution of unilamellar vesicles were determined by photon correlation spectroscopy (PCS). A PCS41 particle size analyser (Malvern Autosizer llc) and a 5 mW He–Ne laser (Spectra Physics), at an excitation wavelength of 633 nm, were used. Data were collected with a Malvern 7032N 72 data channel correlator and the mean hydrodynamic diameter was calculated from a cumulant analysis of the intensity autocorrelation function. Before measuring, vesicle dispersions were appropriately diluted to avoid multiple scattering. The influence of such dilution on size measurement has been previously proved to be non-significant (unpublished results). Size determinations at different periods of time after liposome preparation were performed to control their stability.

To control the stability of the liposomal suspensions the size and size distribution of unilamellar vesicles were also determined by PCS at 24 and 168 h after liposome preparation. Besides, the stability of liposomes was also checked by measuring the porphyrin content in liposomes at 24 and 168 h after liposome preparation, by means of the disruption of the liposomes (free of non-entrapped porphyrin) and by the measure of the absorption as indicated in the preceding section.

2.5. Differential scanning calorimetry

Calorimetric measurements were carried out by a Mettler DSC-30 differential scanning calorimeter. The temperature of the maximum of the transition endotherm (T_m) and the enthalpy (ΔH_{cal}) were determined with a Mettler TC10A TA processor. The processor analyses the heat flow curves obtained during dynamic experiments by integration of the area under the peak over a dynamic baseline, type X8. ΔS_{cal} was obtained as $\Delta H_{cal}/T_m$. The cooperativity of the transition was evaluated, in an approximate manner, from the widths at half-peak heights (°C) of the main transition endotherms ($\Delta T_{1/2}$). Fifteen milligram of lipid, in the absence and in the presence of porphyrin, were transferred to a 160-μl aluminium sample pan as THF solution. THF was evaporated with a nitrogen stream and the calorimetric pans with the film were kept in a vacuum desiccator for 12 h over $CaCl_2$. One hundred microliter of a 50 mM imidazole–HCl buffer (pH 7.4)-ethylene glycol (1:1, v/v) mixture were added to the pans to hydrate the films. Fifty percent ethylene glycol was added to the

Table 1
Effect of lipid in the molar absorption coefficients and in the Soret bands characteristics of tetraphenyl and tetrapyridyl porphyrins

Molar ratio	Sample	ε[a] ($M^{-1}\,cm^{-1}$)	λ_{max} (nm)	$\nu_{1/2}$[b] (nm)
0:0:1	POPC/OOPS/TPP	$(4.16 \pm 0.02) \times 10^5$	416.0 ± 0.4	11.8 ± 0.3
	POPC/OOPS/ZnTPP	$(6.08 \pm 0.01) \times 10^5$	423.2 ± 0.6	10.2 ± 0.2
	POPC/OOPS/MnTPP	$(11.70 \pm 0.10) \times 10^4$	474.0 ± 1.0	16.9 ± 0.3
	POPC/OOPS/ZnTPyP	$(2.87 \pm 0.02) \times 10^5$	425.0 ± 0.5	13.5 ± 0.4
13.5:1.5:1	POPC/OOPS/TPP	$(4.78 \pm 0.04) \times 10^5$	415.8 ± 0.5	11.8 ± 0.2
	POPC/OOPS/ZnTPP	$(6.38 \pm 0.01) \times 10^5$	422.8 ± 0.6	10.2 ± 0.3
	POPC/OOPS/MnTPP	$(9.82 \pm 0.04) \times 10^4$	475.0 ± 1.0	20.3 ± 0.2
	POPC/OOPS/ZnTPyP	$(2.50 \pm 0.03) \times 10^5$	424.6 ± 0.4	13.5 ± 0.1
36:5:1	POPC/OOPS/TPP	$(4.75 \pm 0.02) \times 10^5$	415.6 ± 0.5	11.8 ± 0.2
	POPC/OOPS/ZnTPP	$(6.78 \pm 0.01) \times 10^5$	422.8 ± 0.6	10.2 ± 0.2
	POPC/OOPS/MnTPP	$(9.62 \pm 0.03) \times 10^4$	474.0 ± 1.0	20.3 ± 0.3
	POPC/OOPS/ZnTPyP	$(2.53 \pm 0.02) \times 10^5$	424.7 ± 0.7	13.5 ± 0.2
90:10:1	POPC/OOPS/TPP	$(4.62 \pm 0.04) \times 10^5$	415.5 ± 0.5	11.8 ± 0.3
	POPC/OOPS/ZnTPP	$(7.28 \pm 0.08) \times 10^5$	423.0 ± 0.6	10.2 ± 0.3
	POPC/OOPS/MnTPP	$(8.83 \pm 0.18) \times 10^4$	473.0 ± 1.0	20.3 ± 0.2
	POPC/OOPS/ZnTPyP	$(2.55 \pm 0.04) \times 10^5$	424.7 ± 0.8	13.5 ± 0.3
0:1	POPC/ZnTPyP	$(2.87 \pm 0.02) \times 10^5$	425.0 ± 0.5	13.5 ± 0.4
15:1		$(3.00 \pm 0.04) \times 10^5$	426.0 ± 1.0	13.5 ± 0.2
40:1		$(3.05 \pm 0.03) \times 10^5$	425.9 ± 1.0	13.5 ± 0.3
100:1		$(3.06 \pm 0.18) \times 10^5$	425.9 ± 1.0	13.5 ± 0.2

[a] For ε determination measures were carried out at the λ_{max} of the Soret band of each porphyrin in THF/50 mM imidazole HCl buffer pH 7.4 (24/1, v/v) using the appropriate porphyrin concentration range, at room temperature.
[b] Width of the Soret band at half peak height. Data are the mean values ± S.D. of three independent experiments.

aqueous phase to prevent freezing of the bulk solvent phase, since the endotherm of the lipid mixture begins below 0 °C. The reference pan contained 100 μl of a 1/1 (v/v) mixture of the same buffer and ethylene glycol. Several heating and cooling cycles were carried out to equilibrate the samples before to run the definitive calorimetric scans. The temperature scale was calibrated with indium, undecane and water and the transition enthalpies were calibrated with indium. The heating rate was 2 °C/min, and only the heating scans were analysed (−40 to 40 °C). After calorimetric scans, the phospholipid amount was determined by lipid phosphorous analysis by the method of Rouser et al. (1970).

2.6. Photophysical studies

Ground state absorption spectra were recorded using a Varian Cary 4E spectrophotometer. Singlet oxygen was monitored in time-resolved experiments via its phosphorescence at 1270 nm using a 77 K Ge detector (North Coast EOL-817P). The 3rd harmonic of a Continuum Surelite Nd:YAG laser was used to pump a Continuum optical parametric oscillator, the output of which, in turn, was used to irradiate the sample (3 mm beam diameter, 5 ns pulsewidth, 0.1–1 mJ per pulse). The detector output was fed to a Lecroy 9410 digital oscilloscope, and acquired by a computer for storage and analysis. To improve signal-to-noise ratios, data recorded from 10–100 independent laser pulses were averaged. For the determination of singlet oxygen quantum yields, the signal amplitude extrapolated to the end of the laser pulse was compared for the samples and for suitable references in air-saturated, optically-matched solutions (Nonell and Braslavsky, 2000). Thus, TPPS with $\Phi_\Delta = 0.66$ (Nardello et al., 1997) and UP with $\Phi_\Delta = 0.48$ (Spikes, 1992) were used as references for D_2O-suspended liposomes, while TPP with $\Phi_\Delta = 0.68$ (Zenkevich et al., 1996) and C_{60} with $\Phi_\Delta = 0.92$ (Terazima et al., 1991) were used in toluene. The value for TPP was assumed to hold for $CHCl_3$:MeOH (2:1) solutions.

3. Results

3.1. Lipid effect on the Soret absorption band of different porphyrins

Table 1 shows the spectroscopic parameters of different tetraphenyl and tetrapyridyl porphyrins in the absence and in the presence of different amounts of lipids. It can be observed that, in general, the molar absorption coefficient of the porphyrins changes when lipid is present in the medium. The λ_{max} and the $\nu_{1/2}$ of the Soret absorption band of TPP, ZnTPP and ZnTPyP were not modified in the presence of lipids. Nevertheless, a broadening was observed for the Soret absorption band of MnTPP in the presence of lipid ($\nu_{1/2}$ from 16.9 to 20.3 nm), irrespective of lipid/porphyrin molar ratio, without a significant modification of λ_{max}.

The effect of lipid on the molar absorption coefficient depends on the porphyrin and lipid nature. An increase in ε for TPP from $4.2 \times 10^{-5}\,M^{-1}\,cm^{-1}$ to ca. $4.7 \times 10^{-5}\,M^{-1}\,cm^{-1}$ was observed in the presence of lipid, irrespective of lipid concentration. A gradual increase in ε takes place when increasing lipid concentration for ZnTTP. For MnTTP, a continuous decrease in the ε value was observed upon increasing the lipid concentration. Finally, the ε value for ZnTPyP showed a little decrease in the presence of POPC/OOPS and a little increase in the presence of POPC, irrespective of lipid concentration.

3.2. Incorporation of Zn and Mn derivatives of tetraphenyl and tetrapyridyl porphyrins into liposomes

The porphyrin concentration in the liposomal systems was estimated spectrophotometrically, as indicated in methods, using for each porphyrin the ε values at the corresponding lipid/porphyrin molar ratio given in Table 1.

Table 2 gives the incorporation efficiency obtained for TPP derivatives. The values at time 0 correspond to the lipid and porphyrin content of the liposomal systems just obtained, whereas the values at 24 and 168 h were estimated to control the stability of such liposomal systems during storage. The data indicate an increase in the percentage of incorporation of ZnTPP and MnTPP with respect to the unmetallated-porphyrin at all lipid/porphyrin molar ratios assayed. Moreover, for all the TPP derivatives assayed the percentage of porphyrin incorporation increases with the initial lipid/porphyrin molar ratio used to obtain the films, being the increase more evident for nonmetalled-TPP with the lowest incorporation efficiency. Nevertheless, the molar concentration of the porphyrin incorporated into the bilayers was higher for the liposomal dispersions obtained at the lowest lipid/porphyrin molar ratio. On the other hand, the lipid amount in all liposomal dispersions was near to 100% (ca. 10 mg lipid/ml liposomal dispersion), irrespective of the initial lipid/porphyrin molar ratio and of the porphyrin nature.

After storage the lipid content remains constant but a significant and time dependent decrease in the percentage of porphyrin incorporation was observed for TPP at all initial lipid/porphyrin molar ratios assayed, indicating the instability of the system. In all cases, after 168 h of storage, the amount of porphyrin in the liposomal suspensions was quite similar and near to 7.0×10^{-5} M, with a ratio of approximately 200 molecules of lipid per molecule of porphyrin. Moreover, the high S.D. values obtained for the liposomal suspensions incorporating TPP were also indicative of the instability of this system.

On the contrary, the amount of lipid in the liposomal dispersions and the percentages of incorporation of MnTPP remained almost constant after 168 h of storage, showing the stability of the systems. For ZnTPP, the lipid content remained constant after storage, but near a 20% decrease in the porphyrin content was observed after 168 h of storage, irrespective of the initial lipid/porphyrin molar ratio. In these cases, after storage, the molar ratio between lipid and porphyrin molecules was almost the same than that used to obtain the initial film, indicating the high efficiency of incorporation of such metallated tetraphenylporphyrins. In addition, the S.D. values for the different parameters related to the liposomal dispersions which incorporate ZnTPP and MnTPP were always $\leq$8%.

Liposomes containing TPP, ZnTPP and MnTPP, at different lipid/porphyrin molar ratio were analysed for size and size distribution by dynamic light scattering. The results are summarised in Table 3. The mean hydrodynamic diameter of porphyrin containing liposomes was almost the same for all systems and remains constant during storage, showing the

Table 2
Incorporation efficiency of tetraphenyl porphyrins in POPC/OOPS liposomes: stability of the liposomal systems

Molar ratio	Sample	Time (h)	L[a] (%)	P[b] (%)	[P] (molar)	L/P[c] (ratio)
13.5:1.5:1	POPC/OOPS/TPP	0	97.1 ± 3.6	20.0 ± 58.1	(1.9 ± 5.5) × 10^{-4}	72.6 ± 40.7
		24	98.6 ± 1.6	13.7 ± 5.7	(1.4 ± 0.6) × 10^{-4}	103.9 ± 25.5
		168	96.6 ± 6.0	8.1 ± 4.9	(7.4 ± 0.5) × 10^{-5}	180.0 ± 53.5
	POPC/OOPS/ZnTPP	0	100.6 ± 0.8	95.7 ± 0.2	(8.4 ± 0.1) × 10^{-4}	15.8 ± 0.2
		24	98.2 ± 0.1	76.4 ± 3.3	(6.7 ± 0.3) × 10^{-4}	19.3 ± 0.9
		168	98.3 ± 0.8	72.5 ± 2.1	(6.4 ± 0.2) × 10^{-4}	20.3 ± 0.7
	POPC/OOPS/MnTPP	0	100.0 ± 0.1	95.3 ± 1.3	(10.1 ± 0.2) × 10^{-4}	15.9 ± 0.4
		24	100.0 ± 0.8	98.1 ± 2.0	(10.4 ± 0.2) × 10^{-4}	15.4 ± 0.1
		168	98.9 ± 0.3	88.6 ± 4.8	(9.3 ± 0.5) × 10^{-4}	16.8 ± 0.8
36:4:1	POPC/OOPS/TPP	0	99.1 ± 1.2	76.6 ± 12.4	(2.4 ± 0.4) × 10^{-4}	51.7 ± 12.3
		24	98.8 ± 0.4	24.8 ± 21.6	(7.7 ± 0.7) × 10^{-5}	159.6 ± 62.4
		168	98.8 ± 0.9	19.2 ± 11.8	(6.0 ± 0.4) × 10^{-5}	206.2 ± 66.5
	POPC/OOPS/ZnTPP	0	97.4 ± 0.6	100.9 ± 0.9	(3.8 ± 0.1) × 10^{-4}	38.1 ± 0.9
		24	99.0 ± 1.3	92.7 ± 8.0	(3.5 ± 0.2) × 10^{-4}	41.7 ± 3.0
		168	96.9 ± 3.8	77.8 ± 5.2	(2.9 ± 0.3) × 10^{-4}	48.7 ± 2.2
	POPC/OOPS/MnTPP	0	102.0 ± 3.6	89.4 ± 5.4	(3.5 ± 0.2) × 10^{-4}	45.7 ± 0.8
		24	97.9 ± 2.7	92.0 ± 4.5	(3.6 ± 0.2) × 10^{-4}	42.6 ± 0.5
		168	97.9 ± 2.4	94.1 ± 1.8	(3.7 ± 0.1) × 10^{-4}	41.8 ± 0.3
90:10:1	POC/OOPS/TPP	0	100 ± 0.8	74.6 ± 25.2	(10.3 ± 3.4) × 10^{-5}	134.0 ± 82.5
		24	99.4 ± 0.3	68.9 ± 21.1	(9.5 ± 2.9) × 10^{-5}	144.2 ± 76.9
		168	99.3 ± 3.1	50.7 ± 16.5	(7.0 ± 2.2) × 10^{-5}	196.0 ± 102.2
	POPC/OOPS/ZnTPP	0	95.7 ± 2.1	99.0 ± 0.7	(9.9 ± 0.2) × 10^{-5}	97.8 ± 0.6
		24	94.3 ± 1.2	84.3 ± 2.1	(8.6 ± 0.2) × 10^{-5}	111.9 ± 1.3
		168	100.8 ± 2.6	82.2 ± 2.9	(8.4 ± 0.3) × 10^{-5}	122.6 ± 7.1
	POPC/OOPS/MnTPP	0	105.3 ± 3.8	102.7 ± 2.4	(2.0 ± 0.1) × 10^{-4}	101.9 ± 0.7
		24	99.7 ± 0.7	99.1 ± 1.3	(1.9 ± 0.1) × 10^{-4}	100.6 ± 0.5
		168	100.4 ± 1.8	99.5 ± 0.3	(1.9 ± 0.1) × 10^{-4}	103.0 ± 3.0

Liposomes were obtained in a 50 mM imidazole–HCl buffer (pH 7.4) at a lipid concentration of 10 mg/ml. The lipid/porphyrin molar ratios, indicated in the top of the table, were those used for liposome preparation. The initial porphyrin content depended on the lipid concentration and on the lipid/porphyrin molar ratio. The values indicated in the table were calculated from the data obtained for lipid and porphyrin content in liposomes, free of non-entrapped porphyrin.

[a] L: lipid content, expressed as the percentage of lipid in the sample with respect to the lipid present at the initial stage of liposome preparation.

[b] P: porphyrin content, expressed as the percentage of porphyrin in the sample with respect to the porphyrin present at the initial stage of liposome preparation.

[c] L/P: lipid/porphyrin molar ratio, which indicates the amount of lipid molecules per molecule of porphyrin in the final liposome dispersion, free of non-entrapped porphyrin. The lipid content of empty liposomes suspensions was shown to be constant during storage, without neither loss nor changes of lipid constituents. Data are the mean values ± S.D. of three independent experiments.

stability of the liposomal systems and that the nature and the amount of porphyrin in the bilayers did not modify the liposome size. The high polydispersity values obtained for these liposomal dispersions can be related to the microemulsification method used to obtain liposomes which, in general, provides liposomal systems less monodisperse than other methodologies like extrusion. A discrepancy in the stability was observed from the measure of lipid and porphyrin content and from size analysis, for TPP-containing liposomes. This discrepancy can be explained by the fact that TPP incorporation into bilayers is difficult and thus, part of the initial non-correct incorporated porphyrin is excluded from the bilayer and precipitates without any significant change in the size of the liposomes.

Table 3
Size and stability control of tetraphenylporphyrins containing liposomes

Sample	Time (h)	Molar ratio					
		13.5:1.5:1		36:4:1		90:10:1	
		Zave[a]	Poly[b]	Zave[a]	Poly[b]	Zave[a]	Poly[b]
POPC/OOPS/TPP	0	180.5 ± 24.1	0.460 ± 0.030	175.5 ± 11.2	0.452 ± 0.030	133.4 ± 0.4	0.478 ± 0.014
	24	177.1 ± 21.2	0.527 ± 0.110	163.5 ± 19.2	0.473 ± 0.020	140.9 ± 9.2	0.474 ± 0.044
	168	171.5 ± 17.1	0.415 ± 0.004	168.3 ± 35.9	0.389 ± 0.070	140.9 ± 18.4	0.407 ± 0.034
POPC/OOPS/ZnTPP	0	174.0 ± 1.0	0.300 ± 0.004	149.8 ± 10.9	0.297 ± 0.008	143.4 ± 2.8	0.597 ± 0.057
	24	168.9 ± 1.8	0.282 ± 0.003	149.8 ± 9.5	0.251 ± 0.050	145.3 ± 2.3	0.610 ± 0.067
	168	160.9 ± 1.6	0.399 ± 0.020	140.6 ± 9.8	0.309 ± 0.060	146.6 ± 2.3	0.431 ± 0.016
POPC/OOPS/MnTPP	0	164.0 ± 3.4	0.441 ± 0.010	167.6 ± 1.0	0.357 ± 0.096	173.0 ± 1.9	0.306 ± 0.010
	24	178.7 ± 1.3	0.313 ± 0.001	173.8 ± 0.7	0.358 ± 0.010	176.1 ± 0.9	0.380 ± 0.001
	168	173.6 ± 1.0	0.353 ± 0.025	179.2 ± 3.7	0.360 ± 0.013	174.1 ± 2.8	0.342 ± 0.018

Liposome diameters, calculated from photon correlation spectroscopy data, for the same liposomal dispersions as those indicated in Table 2.
[a] *Z* average mean.
[b] Polydispersity: *Z* average mean and polydispersity values for POPC/OOPS empty liposomes were 105 ± 5.3 nm and 0.352 ± 0.05 nm. Data are the mean values ± S.D. of three independent experiments.

The incorporation efficiency of ZnTPyP in POPC/OOPS and POPC liposomes is given in Table 4. The results for nonmetallated-TPyP are not shown since the incorporation efficiency of this porphyrin was very small. The initial percentage of incorporation of TPyP in POPC/OOPS and POPC liposomes was independent on the initial lipid/porphyrin molar ratio and was as small as 4%. Moreover, after 1 week of storage, the remaining porphyrin in liposomes was less than 2%. This result indicates that the substitution of the phenyl groups in *meso* by pyridyl groups causes a dramatic decrease in the incorporation efficiency. The introduction of Zn into the porphyrinic ring of TPyP increases the incorporation efficiency of the porphyrin. The percentage of incorporation increases with the lipid/porphyrin molar ratio both for liposomes obtained with POPC/OOPS mixtures and POPC, being the porphyrin incorporation efficiency slightly higher in POPC liposomes at the lipid/porphyrin molar ratios of 40:1 and 100:1. The lipid content of the liposomal systems just obtained ranged, in general, between 93 and 97%. Storage only causes a little decrease in lipid and porphyrin content for all the liposomal systems, showing their considerable stability. Nevertheless, the S.D. values for the porphyrin content and for the L/P molar ratio in the liposomal systems obtained from an initial 90:10:1 POPC/OOPS/ZnTPyP mixture, indicate a high dispersion of the experimental values and suggest that the incorporation of ZnTPyP in such bilayers is not easy. After storage, the concentration of ZnTPyP in the POPC/OOPS liposomal systems decreased from 7.7×10^{-5} to 3.2×10^{-5} M when increasing the initial lipid/porphyrin molar ratio. Nonetheless, for POPC liposomes the concentration of ZnTPyP was in all cases the same and gives a final lipid/porphyrin molar ratio of 142. Thus, the inclusion of OOPS in the lipid bilayer, despite slightly increasing the fluidity of the bilayer, does not improve ZnTPyP incorporation into bilayers.

Table 5 shows the size and size distribution of POPC/OOPS and POPC liposomes containing ZnTPyP, at different lipid/porphyrin molar ratio. The mean hydrodynamic diameter of porphyrin containing POPC/OOPS liposomes was a bit smaller than that of porphyrin containing POPC liposomes. This different size can account for the smallest incorporation efficiency observed for ZnTPyP in POPC/OOPS liposomes as a consequence of the biggest curvature radium. In all cases, the size was almost independent of the initial lipid/porphyrin molar ratio and remains constant during storage, showing the stability of the liposomal systems and that the amount of porphyrin in the bilayers did not modify the liposome size.

Table 4
Incorporation efficiency of Zn-tetrapyridyl porphyrin in POPC/OOPS and POPC liposomes: stability of the liposomal systems

Sample	Molar ratio	Time (h)	L[a] (%)	P[b] (%)	[P] (molar)	L/P[c] (ratio)
POPC/OOPS/ZnTPyP	13.5:1.5:1	0	99.7 ± 0.8	16.4 ± 3.8	(9.8 ± 1.2) × 10^{-5}	91.0 ± 18.2
		24	98.4 ± 0.5	16.8 ± 4.1	(10.0 ± 1.4) × 10^{-5}	88.2 ± 14.7
		168	97.6 ± 1.2	13.0 ± 3.5	(7.7 ± 1.5) × 10^{-5}	113.1 ± 16.2
	36:4:1	0	97.4 ± 1.1	17.6 ± 3.3	(6.1 ± 1.1) × 10^{-5}	221.0 ± 59.4
		24	99.2 ± 0.4	19.2 ± 3.1	(6.6 ± 1.1) × 10^{-5}	207.1 ± 41.7
		168	83.2 ± 10.3	17.1 ± 4.5	(6.9 ± 1.6) × 10^{-5}	195.0 ± 12.1
	90:10:1	0	97.8 ± 0.1	35.1 ± 13.4	(3.6 ± 1.4) × 10^{-5}	279.0 ± 230.5
		24	95.8 ± 0.9	33.4 ± 13.2	(3.4 ± 1.4) × 10^{-5}	287.1 ± 260.2
		168	97.1 ± 0.7	30.8 ± 12.4	(3.2 ± 1.3) × 10^{-5}	315.2 ± 301.0
POPC/ZnTPyP	15:1	0	93.4 ± 0.9	14.4 ± 2.40	(7.7 ± 1.3) × 10^{-5}	129.8 ± 32.1
		24	88.1 ± 5.2	15.8 ± 3.4	(8.5 ± 1,8) × 10^{-5}	111.0 ± 18.2
		168	90.1 ± 0.3	12.7 ± 0.1	(6.8 ± 0.1) × 10^{-5}	142.2 ± 0.8
	40:1	0	94.4 ± 0.9	36.7 ± 3.8	(9.0 ± 0.7) × 10^{-5}	102.8 ± 6.1
		24	90.6 ± 2.5	33.1 ± 3.4	(8.1 ± 0.8) × 10^{-5}	109.6 ± 6.6
		168	96.6 ± 0.3	27.4 ± 0.9	(6.7 ± 0.2) × 10^{-5}	141.3 ± 6.7
	100:1	0	93.4 ± 1.3	74.6 ± 0.8	(7.7 ± 0.5) × 10^{-5}	129.8 ± 6.1
		24	88.1 ± 3.4	73.8 ± 1.1	(7.7 ± 0.8) × 10^{-5}	125.5 ± 5.3
		168	90.1 ± 2.4	65.8 ± 0.6	(6.8 ± 0.3) × 10^{-5}	142.2 ± 4.8

The experimental conditions were the same as those indicated in Table 2.
[a] L: lipid content, expressed as the percentage of lipid in the sample with respect to the lipid present at the initial stage of liposome preparation.
[b] P: porphyrin content, expressed as the percentage of porphyrin in the sample with respect to the porphyrin present at the initial stage of liposome preparation.
[c] L/P: lipid/porphyrin molar ratio, which indicates the amount of lipid molecules per molecule of porphyrin in the final liposome dispersion, free of non-entrapped porphyrin. The lipid content of empty liposomes suspensions was shown to be constant during storage, without neither loss nor changes of lipid constituents. Data are the mean values ± S.D. of three independent experiments.

Table 5
Size and stability control of Zn-tetrapyridyl porphyrin containing liposomes

Sample	Time (h)	Molar ratio					
		13.5:1.5:1		36:4:1		90:10:1	
		Zave[a]	Poly[b]	Zave[a]	Poly[b]	Zave[a]	Poly[b]
POPC/OOPS/ZnTPyP	0	146.6 ± 2.6	0.495 ± 0.010	149.6 ± 7.9	0.513 ± 0.100	149.2 ± 31.5	0.489 ± 0.003
	24	143.5 ± 2.1	0.443 ± 0.033	136.3 ± 9.1	0.514 ± 0.057	139.5 ± 27.0	0.515 ± 0.076
	168	132.0 ± 4.8	0.363 ± 0.033	134.6 ± 6.2	0.464 ± 0.068	139.5 ± 28.7	0.518 ± 0.061
		15:1		40:1		100:1	
		Zave[a]	Poly[b]	Zave[a]	Poly[b]	Zave[a]	Poly[b]
POPC/ZnTPyP	0	185.2 ± 13.4	0.360 ± 0.015	190.2 ± 11.2	0.350 ± 0.076	174.2 ± 14.2	0.366 ± 0.090
	24	187.1 ± 9.3	0.380 ± 0.021	189.2 ± 10.6	0.320 ± 0.015	175.4 ± 12.3	0.320 ± 0.052
	168	179.7 ± 11.5	0.320 ± 0.028	183.6 ± 13.5	0.330 ± 0.023	177.3 ± 12.8	0.340 ± 0.083

Liposome diameters, calculated from photon correlation spectroscopy data, for the same liposomal dispersions as those indicated in Table 4.
[a] *Z* average mean.
[b] Polydispersity: *Z* average mean and polydispersity values for POPC/OOPS or POPC empty liposomes were, respectively, 105 ± 5.3 nm and 0.352 ± 0.05 nm or 115 ± 8.4 nm and 0.337 ± 0.06 nm. Data are the mean values ± S.D. of three independent experiments.

3.3. Thermotropic properties of liposomes containing tetraphenyl and tetrapyridyl porphyrins

Differential scanning calorimetry was used to determine the effect of the incorporation of tetraphenyl and tetrapyridyl porphyrins in the thermotropic behaviour of the liposomal bilayers. The endothermic transition profiles, obtained for the lipid dispersions in the absence and in the presence of the porphyrins at the indicated molar ratios, showed in all cases a single endotherm. The thermodynamic parameters corresponding to the thermograms are given in Table 6. The transition temperatures obtained showed no significant differences due to the incorporation of TPP, TPyP and ZnTPyP with regard to that of the standard lipid formulation. However, the incorporation of ZnTPP and MnTPP into the bilayers caused, respectively, a decrease and an increase in the main transition temperature, which was independent on the amount of porphyrin incorporated into the bilayer. The thermodynamic parameters ΔH_{cal} and ΔS_{cal} remain almost constant for all the systems. The $\Delta T_{1/2}$ parameter showed a significant increase for bilayers containing ZnTPP and ZnTPyP at all molar ratios and for MnTPP at the lowest lipid/porphyrin molar ratio. These results indicate that the incorporation of porphyrins into the bilayers does not introduce significant changes in the bilayer organisation and does not modify the energy of the transitions. Moreover, an interaction between the lipids and the porphyrins, with high efficiency of incorporation into the liposomal bilayers, can be suggested from the modification of the T_m values and the decrease in the cooperativity of the transition.

3.4. Singlet oxygen quantum yields

The efficiency of a photosensitiser depends on its ability to give singlet oxygen when irradiate with visible or near visible light in the presence of oxygen. In the literature there are referenced Φ_Δ values for a large number of porphyrins in solution (Venediktov and Krasnovsky, 1982; Verlhac et al., 1984; Tanielian and Wolff, 1995; Kruk et al., 1998). Nevertheless, the hydrophobic nature of many of these molecules

Table 6
Effect of tetraphenyl and tetrapyridyl porphyrins liposome incorporation on the thermodynamic parameters of the aqueous dispersions of POPC/OOPS bilayers

POPC/OOPS/porphyrin (molar ratio)	Porphyrin	T_m[a] (°C)	ΔH_{cal}[b] (kJ mol^{-1})	ΔS_{cal}[c] (kJ mol^{-1} K^{-1})	$\Delta T_{1/2}$[d] (°C)
90:10:1	None	−5.1 ± 0.7	17.5 ± 0.9	65.3 ± 3.2	4.9 ± 0.4
	TPP	−5.2 ± 0.2	18.4 ± 0.2	68.7 ± 0.7	4.9 ± 0.2
	ZnTPP	−6.2 ± 0.1	17.6 ± 0.5	65.9 ± 1.8	5.5 ± 0.2
	MnTPP	−3.8 ± 0.2	17.6 ± 0.7	65.4 ± 2.5	4.7 ± 0.2
	TPyP	−5.4 ± 0.7	17.0 ± 0.1	63.5 ± 0.4	5.1 ± 0.1
	ZnTPyP	−5.7 ± 0.1	17.6 ± 0.2	65.8 ± 0.7	5.6 ± 0.4
36:4:1	None	−5.1 ± 0.7	17.5 ± 0.9	65.3 ± 3.2	4.9 ± 0.4
	TPP	−5.0 ± 0.1	17.8 ± 0.1	66.4 ± 0.4	4.8 ± 0.1
	ZnTPP	−6.7 ± 0.3	17.0 ± 0.3	63.8 ± 1.1	5.9 ± 0.3
	MnTPP	−3.8 ± 0.6	17.0 ± 0.6	63.2 ± 2.2	4.9 ± 0.1
	TPyP	−5.5 ± 0.1	16.8 ± 0.3	62.8 ± 1.1	4.9 ± 0.1
	ZnTPyP	−5.7 ± 0.1	17.0 ± 0.2	63.6 ± 0.7	5.8 ± 0.1
13.5:1.5:1	None	−5.1 ± 0.7	17.5 ± 0.9	65.3 ± 3.2	4.9 ± 0.4
	TPP	−5.2 ± 0.1	17.3 ± 0.1	64.6 ± 0.4	4.8 ± 0.1
	ZnTPP	−6.4 ± 0.2	16.6 ± 0.1	62.3 ± 0.03	5.7 ± 0.1
	MnTPP	−4.5 ± 0.9	17.0 ± 0.2	63.3 ± 0.7	5.8 ± 0.2
	TPyP	−5.5 ± 0.1	17.3 ± 0.4	64.7 ± 1.5	5.1 ± 0.1
	ZnTPyP	−5.7 ± 0.1	16.7 ± 0.4	62.5 ± 1.5	6.1 ± 0.1

[a] Temperature corresponding to the maximum of the calorimetric peak.
[b] Calorimetric enthalpy calculated from the area under the peak.
[c] Calorimetric entropy calculated as $\Delta H_{cal}/T_m$.
[d] Width of the calorimetric peak at half peak height. Data are the mean values ± S.D. of three independent experiments.

Table 7
Singlet oxygen production quantum yields

Sensitizer	Medium	λ_{exc}[a] (nm)	Φ_Δ[b] (this work)	Φ_Δ (literature)
ZnTPP	Toluene	532, 591	0.86 ± 0.09	0.83 (Tanielian and Wolff, 1995)
ZnTPP	POPC/OOPS/D_2O	560	0.51 ± 0.05	–
MnTPP	Toluene	532, 591	0.003 ± 0.001	<0.01 (Venediktov and Krasnovsky, 1982)
TpyP	Toluene	532, 591	0.85 ± 0.09	0.9 (Kruk et al., 1998)[c]
TpyP	$CHCl_3$:MeOH (2:1)	516, 591	0.77 ± 0.08	0.9 (Kruk et al., 1998)[c]
ZnTPyP	Toluene	532, 591	0.80 ± 0.08	0.88 (Verlhac et al., 1984)[c]
ZnTPyP	$CHCl_3$:MeOH (2:1)	516, 591	0.81 ± 0.08	0.88 (Verlhac et al., 1984)[c]

[a] Excitation wavelength.
[b] TPP with $\Phi_\Delta = 0.68$ (Zenkevich et al., 1996) and C_{60} with $\Phi_\Delta = 0.92$ (Terazima et al., 1991) were used as standards in toluene. TPPS with $\Phi_\Delta = 0.66$ (Nardello et al., 1997) and UP with $\Phi_\Delta = 0.48$ (Spikes, 1992) were used as standards in the liposome suspensions. TPP was used as standard in $CHCl_3$:MeOH 2:1, assuming $\Phi_\Delta = 0.66$.
[c] Literature values refer to the tetra-*N*-methylated sensitizers in D_2O.

states the need of solubilising systems that allow their systemic administration, like lipid-based delivery systems, i.e. liposomes (Vion-Dury et al., 1989; Sorin et al., 1995). The efficiency of singlet oxygen production by the photosensitizers can hence be modified due to the organised lipid environment, which replaces solvent molecules. To assess the effect of liposome incorporation onto singlet oxygen production by our porphyrins, we determined its quantum yield by means of time-resolved near-infrared phosphorescence detection. The production of singlet oxygen by the photosensitisers was assessed by means of time-resolved near-infrared phosphorescence detection. The results are collected in Table 7.

The quantum yield values obtained for tetraphenylporphyrins in toluene compare favourable to those in the literature. The data for tetrapyridyl porphyrins are new and the values found in neat solvents are similar to those of the corresponding tetra-*N*-methylated porphyrins. Interestingly, the free base TPyP is a better photosensitiser than TPP, while the Zn(II) complexes behave similarly.

Taken into account the values of Φ_Δ obtained in organic solvents (Table 7) and the incorporation efficiency of porphyrins into liposomes (Tables 2 and 4), we have also determined Φ_Δ values for ZnTPP in a liposomal media. As can be seen in Table 7, the incorporation of ZnTPP into POPC/OOPS liposomes results in a decrease in its Φ_Δ, from 0.86 in toluene to 0.51. Thus, although this is a reduction of about 40% in the Φ_Δ value for ZnTPP when incorporated into liposomes, the value obtained seems to be high enough to use liposomal formulations of this photosensitiser to generate singlet oxygen.

The absorption spectra of ZnTPP in THF and incorporated into POPC/OOPS liposomes are shown in Fig. 1. Liposomes containing ZnTPP were prepared in

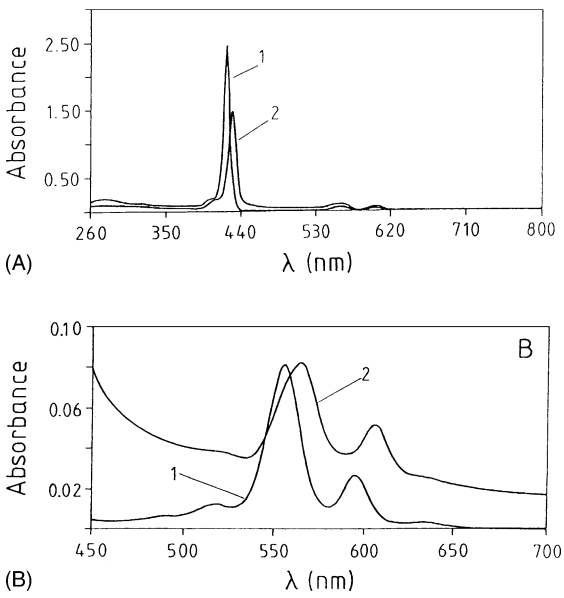

Fig. 1. Absorption spectra of POPC/OOPS/ZnTPP (13.5:1.5:1) in THF (1) and absoption spectra of POPC/OOPS/ZnTPP (13.5:1.5:1) liposomes in 50 mM imidazole–HCl buffer, pH = 7.4 (2). In both samples lipid and porphyrin concentrations were 163.4 and 10.42 μM, respectively. The figure shows the whole spectra of ZnTPP in liposomes and in toluene solution (A) and a magnification of the corresponding Q-bands zones (B).

D_2O at 10 mg lipid/ml. Twenty-five microliters of the POPC/OOPS/ZnTPP (13.5:1.5:1) liposomal suspension were diluted to 2 ml with 50 mM imidazole–HCl buffer, pH 7.4, or THF, in order to get the same ZnTPP amount in both samples. The porphyrin concentration has been calculated taking into account its percentage of incorporation into liposomes (95.7%). A decrease in the absorption and a shift to a higher λ value for the Soret band of ZnTPP was observed when incorporated into liposomal bilayers. Moreover, Q-bands were also shifted to higher λ values. These results, and the fact that ZnTPP incorporated into liposomes generates singlet oxygen, suggest that ZnTPP is incorporated into the bilayers in a monomeric form and that the change observed for its spectrum depends on the interaction of the dye with the neighbouring lipids in the bilayer.

4. Discussion

The benefits of photodynamic therapy have been reviewed in the literature (Henderson and Dougherty, 1992; Bonnett, 1995; Dougherty et al., 1998; Oleinick and Evans, 1998; Kessel and Dougherty, 1999). The potential applications of the photodynamic effect include cancer chemotherapy, virucidal and bactericidal activity and microbicidal action (Ben-Hur and Horowitz, 1996; Love et al., 1996; Verma et al., 1998; Morgan and Oseroff, 2001). Moreover, some macrocyclic compounds can be used for cancer diagnostics by MRI (Brockhorst et al., 1994).

How photodynamic therapy works has been the subject of many investigations and two possible mechanisms have been proposed. In both of them, the ability of the photosensitiser used to give reactive oxygenated products plays a pivotal role, but there is much indirect evidence to suggest that singlet oxygen, generated through type II mechanism, is the major damaging species produced (Henderson and Dougherty, 1992; Bonnett, 1995). Nevertheless and irrespectively of the used mechanism, it will be necessary to achieve the interaction of the photosensitisers with biological structures in order to internalise them in those cells that need to be treated or visualised. Moreover, it will also be necessary to have suitable pharmaceutical formulations to supply the therapeutic or diagnostic agents by the administration routes often used. In addition, it must be considered that, after incorporation into liposomes, the sensitiser should maintain its ability to form singlet oxygen. All these considerations have been taken into account to plan the experimental work reported here and thus, the main goal of this paper has been the design of liposomal vehicles to incorporate photoactive agents and stable enough to be considered as a realistic alternative to conventional pharmaceutical forms.

The incorporation of photosensitisers into liposomes needs a careful consideration of the natural tendency of these molecules towards aggregation states, which in addition are favoured by certain solvents. If porphyrins aggregate because of or during the incorporation process into lipid bilayers, sensitiser-rich domains would be formed with the resulting phase separation from lipid constituents and the consequent heterogeneity into the hydrophobic core of the bilayer. Moreover, the size of such aggregates would exceed the bilayer thickness, in which case aggregated molecules could be excluded from the bilayer.

The present paper reports the structural photosensitiser features that allow the preparation of stable liposomal formulations, without the undesirable formation of molecular aggregates and gives a rigorous and systematic analysis of the characteristic parameters of the liposomal formulations. Moreover a study in depth of the interaction of the photosensitisers with bilayer lipids by means of the consideration of the possible changes either in the spectroscopic photosensitiser properties or in the thermodynamic parameters of the lipid bilayers have been carried out.

There were considered different lipid/porphyrin ratios in order to achieve the optimal incorporation efficiency and to procure liposomal preparations containing porphyrin concentrations adequate to necessary doses. The amount of the unmetallated porphyrin TPP into liposome bilayers decreases with liposome storage, being its content about one molecule of porphyrin for each two hundred lipid molecules after one week of storage, irrespective of the initial lipid/porphyrin molar ratio. This result suggests a saturation of the lipid bilayer with the porphyrin. Nevertheless, using other porphyrins, like ZnTPP or MnTPP, stable porphyrin-containing liposomes were obtained, irrespective of the initial lipid/porphyrin molar ratio, but higher amounts of porphyrin were incorporated when decreasing the initial lipid/porphyrin molar ratio. The amount of ZnTPP and MnTPP

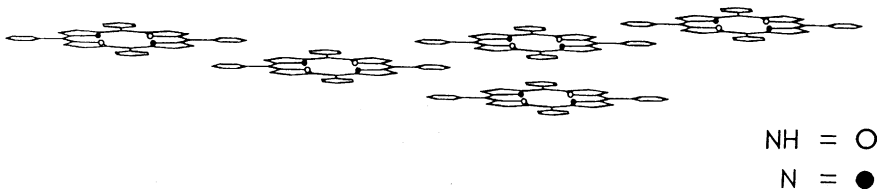

Fig. 2. Aggregates of TPP molecules by π–π interactions between the orbitals of neighbouring molecules.

into liposomes was one molecule of porphyrin for each 15–20 molecules of lipid when the initial lipid/porphyrin molar ratio was 15:1 and this amount remains almost constant after one week of storage.

The results, and the bibliographic data which indicate the formation of porphyrin aggregates (23–26), suggest that, in a watery medium, TPP tends to form aggregates, according to the model indicated in Fig. 2, by π–π interactions between neighbouring porphyrins. The tendency of TPP to aggregate suggests the occurrence of a competition between its interaction with the bilayer and the formation of aggregates. Thus, some of the initial porphyrin molecules incorporated into the bilayer that form aggregates are excluded from the bilayer and precipitate. Nevertheless, porphyrin molecules separate enough will lose their tendency to aggregate and will remain in the liposomal bilayer. The presence of Zn(II) and Mn(III) in the aromatic ring of TPP leads to structural changes, hindering the formation of aggregates (Fig. 2) and increasing the incorporation efficiency of porphyrin into liposomes. The higher incorporation efficiency of MnTPP than ZnTPP can be explained taking into consideration that the Mn volume can be increased by reacting through its axial position and, thus, the tendency of the metallated TPP to form aggregates can be avoided.

The very small incorporation efficiency of TPyP and the little incorporation efficiency of ZnTPyP can be also explained by their tendency to form aggregates. TPyP can form aggregates, like TPP (Fig. 2), through an aggregation characterised by π–π interactions. As it has been indicated, the metal hinders aggregates formation of metallated tetraphenyl porphyrins. Nevertheless, the pyridyl groups in *meso* present in TpyP, with high electronegative character, can favour the formation of aggregates due to the electrostatic interaction between opposite charged groups (Fig. 3) and difficult the efficient incorporation of ZnTPyP into liposomal bilayers.

In a previous paper we show that the presence of Gd in the porphyrinic ring gives high encapsulation efficiencies for both, GdTPP and GdTPyP (Berezin et al., 1997). The high incorporation efficiency of gadolinium porphyrins into the bilayers can also be related

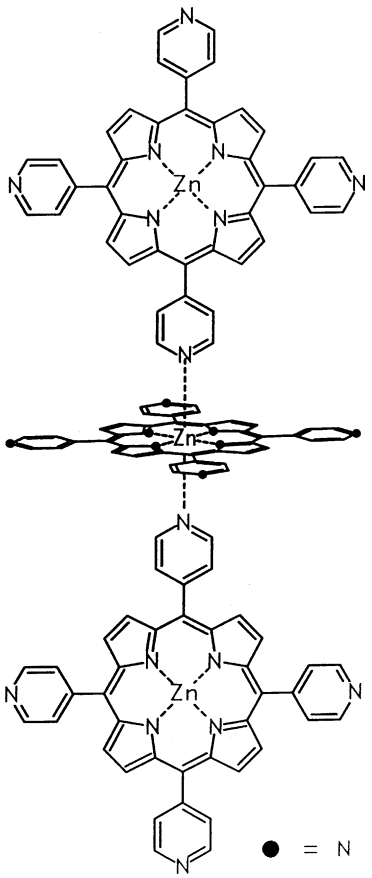

Fig. 3. Aggregates of ZnTPyP molecules by electrostatic interactions of the axial pyridyl groups of ZnTPyP with the metal.

with the low ability of such porphyrins to aggregate. For GdTPP the metal avoids the formation of aggregates in a similar way as Zn and Mn do in ZnTPP and MnTPP, respectively. The presence of gadolinium in GdTPyP will not only difficult the formation of aggregates by π–π interactions (Fig. 2) but also electrostatic aggregates (Fig. 3).

Thus, we can relate the low incorporation efficiency of porphyrins with their ability to form aggregates in a watery media. In this way, the synthesis of hydrophobic porphyrin derived structures or other sensitisers, without tendency to aggregate in a watery media, will be necessary for their efficient incorporation into liposomal bilayers. Moreover, the clinical destination of the photosensitiser, like virus sterilisation of blood, will determine the synthesis of photosensitiser compounds with a displacement of Q-bands to higher λ values.

On the other hand, the incorporation of photosensitisers into liposomal bilayers for therapeutic purposes must preserve their ability to generate singlet oxygen. In this way, we demonstrate the efficient generation of this reactive specie by ZnTPP incorporated into liposomes, although a reduction of the Φ_Δ value for ZnTPP was observed when incorporated into liposomal bilayers. Moreover, a decrease in the absorption and a shift to a higher λ value for the Soret band of ZnTPP was observed when incorporated into liposomal bilayers and Q-bands were shifted to higher λ values. The aggregation state of porphyrins plays a crucial role when these dyes are used as photosensitisers for therapeutic purposes and it has been indicated that only monomeric species and possible planar aggregates, observed in liposomal and mitochondrial membranes, are endowed with significant photosensitising ability (Ricchelli, 1995; Ricchelli et al., 1998). Porphyrin monomers show a significant fluorescence, with two bands between 520 and 690 nm, depending on the structure of the dye and the solvent, but these properties drastically change upon aggregation with very low fluorescence lifetimes (Ricchelli et al., 1998). The whole of the results suggest that ZnTPP is incorporated into the bilayers in a monomeric form and that the change observed for its spectrum depends on the interaction of the dye with the neighbouring lipids in the bilayer. In this way, Ricchelli et al. have also published how the porphyrin-liposome interactions are affected by the physical state of lipid bilayers (Ricchelli et al., 1988). Experimental evidences in favour of this fact include (1) the little incorporation efficiency into liposomes observed for porphyrins with high ability to form aggregates, (2) the high incorporation efficiency into liposomal bilayers observed for ZnTPP, (3) the absorption spectrum and Φ_Δ value obtained for ZnTPP incorporated into liposomal bilayers and (4) the half-life of 60–70 μs measured for singlet oxygen generated by liposomal ZnTPP, characteristic of hydrosoluble photosensitizers in D_2O. The gradual change observed for the molar absorption coefficient of ZnTPP in the presence of increasing amounts of lipid and the modification of the thermodynamic parameters T_m and $\Delta T_{1/2}$ for POPC/OOPS bilayers in the presence of ZnTPP account for the existence of an interaction between ZnTPP and the lipids in the bilayer.

Acknowledgements

This work was supported by grants from the EUROPEAN COMISSION inside the INCO-COPERNICUS 97/98 program (ERBIC15-CT98-0326) and from the Spanish MCyT (SAF2002-04034-C02-02), and by a predoctoral fellowship from the University of Barcelona.

References

Abós, P., Artigas, C., Bertolotti, S., Braslavsky, S.E., Fors, P., Lang, K., Nonell, S., Rodríguez, F.J., Sesé, M.L., Trull, F.R., 1997. Polymer-bound pyrrole compounds, IX. Photophysical and singlet molecular oxygen photosensitizing properties of mesoporphyrin IX covalently bound to a low molecular weight polyethylene glycol. J. Photochem. Photobiol. B: Biol. 41, 53–59.

Akins, D.L., Zhu, H., Guo, C., 1996. Aggregation of tetraaryl-substituted porphyrins in homogeneus solution. J. Phys. Chem. 100, 5420–5425.

Ben-Hur, E., Geacintov, N.E., Studamire, B., Kenney, M.E., Horowitz, B., 1995. The effect of irradiance on virus sterilization and photodynamic damage in red blood cells sensitized by phthalocyanines. Photochem. Photobiol. 61, 190–195.

Ben-Hur, E., Horowitz, B., 1996. Virus inactivation in blood. AIDS 10, 1183–1190.

Berezin, D.B., Bonnett, R., De Madariaga, M.A., Molina, S., Mora, M., Sagristá, M.L., Vallés, M.A., 1997. Gd-meso-tetraphenylporphyrins: synthesis, encapsulation into liposomes and characterization of the resulting preparations. In: Berg, K., Ehrenberg, B., Malic, Z., Moan, J. (Eds.), Photochemotherapy:

Photodynamic Therapy and Other Modalities III. Proceedings of SPIE Series, vol. 3191. SPIE, Bellingham, Washington, pp. 359–367.

Bonnett, R., 1995. Photosensitizers of the porphyrin and phtalocyanine series for photodynamic therapy. Chem. Soc. Rev. 24, 19–33.

Bonnett, R., 2000. Chemical Aspects of Photodynamic Therapy. Gordon and Breach Science Publishers, Amsterdam, pp. 115–128.

Boyle, R.W., Dolphin, D., 1996. Structure and biodistribution relationships of photodynamic sensitizers. Photochem. Photobiol. 64, 469–485.

Brockhorst, K., Els, T., Hoelin-Berlage, M., 1994. Selective enhancement of experimental rat brain tumors with Gd-TPPS. J. Mag. Res. Imaging 4, 451–456.

Dougherty, T.J., Gomer, C.J., Henderson, B.W., Jori, G., Kessel, D., Korbelik, M., Moan, J., Peng, Q., 1998. Photodynamic therapy. J. Natl. Cancer Inst. 90, 889–905.

Henderson, B.W., Dougherty, T.J., 1992. How does photodynamic therapy work? Photochem. Photobiol. 55, 145–157.

Hoebeke, M., 1995. The importance of liposomes as models and tools in the understanding of photosensitization mechanisms. J. Photochem. Photobiol. B: Biol. 28, 189–196.

Hunter, C.A., Sanders, J.K.M., 1990. The nature of π–π interactions. J. Am. Chem. Soc. 112, 5525–5534.

Kessel, D., Dougherty, T.J., 1999. Agents used in photodynamic therapy. Rev. Contemp. Pharmacother. 10, 19–24.

Kruk, N.N., Dzhagarov, B.M., Galievsky, V.A., Chirvony, V.S., Turpin, P.-Y., 1998. Photophysics of the cationic 5,10,15,20-tetrakis(4-*N*-methylpyridyl) porphyrin bound to DNA, [poly(dA-dT]2 and [poly(dG-dC)2]: interaction with molecular oxygen studied by porphyrin triplet–triplet absorption and singlet oxygen luminescence. J. Photochem. Photobiol. B Biol. 42, 181–190.

Love, W.G., Duk, S., Biolo, R., Jori, G., Taylor, P.W., 1996. Liposome-mediated delivery of photosensitizers: localization of zinc (II)-phthalocyanine within implanted tumors after intravenous administration. Photochem. Photobiol. 63, 656–661.

Micali, N., Romeo, A., Lauceri, R., Purrello, R., Mallamace, F., Scolaro, L.M., 2000. Fractal structures in homo- and hetero-aggregated water soluble porphyrins. J. Phys. Chem. B. 104, 9416–9420.

Moan, J., 1990. On the diffusion length of singlet oxygen in cells and tissues. J. Photochem. Photobiol. B: Biol. 6, 343–344.

Morgan, J., Oseroff, A.R., 2001. Mitochondria-based photodynamic anti-cancer therapy. Adv. Drug Delivery. Rev. 49, 71–86.

Müller-Breitkreutz, K., Mohr, H., Briviba, K., Sies, H., 1995. Inactivation of viruses by chemically and photochemically generated singlet molecular oxygen. J. Photochem. Photobiol. B: Biol. 30, 63–70.

Nardello, V., Brault, D., Chavalle, P., Aubry, J.-M., 1997. Measurement of photogenerated singlet oxygen ($^1O_2(^1\Delta_g)$) in aqueous solution by specific chemical trapping with sodium 1,3-cyclohexadiene-1,4-diethanoate. J. Photochem. Photobiol. B Biol. 39, 146–155.

Niesman, M.R., Khoobehi, B., Magin, R.L., Webb, A.G., 1994. Liposomes and diagnostic imaging: the potential to visualize both structure and function. J. Lipos. Res. 4, 741–768.

Nonell, S., Braslavsky, S.E., 2000. Time-resolved singlet oxygen detection. In: Packer, L., Sies, H. (Eds.), Singlet Oxygen, UV-A and Ozone, Methods in Enzymology, vol. 319. pp. 37–49.

North, J., Neyndorff, H., Levy, J.G., 1993. Photosensitizers as virucidal agents. J. Photochem. Photobiol. B: Biol. 17, 99–108.

Oleinick, N.L., Evans, H.H., 1998. The photobiology of photodynamic therapy: cellular targets and mechanisms. Radiat. Res. 150, S146–S156.

Oku, N., 1991. Liposomes. In: Dunn, R., Ottrnbrite, R. (Eds.), Polymeric Drugs and Drug Delivery Systems, ACS Symposium Series, vol. 469. American Chemical Society, Washington, pp. 24–33.

Oku, N., Namba, Y., Okada, S., 1992. Tumor accumulation of novel RES-avoiding liposomes. Biochim. Biophys. Acta 1126, 255–260.

Reddi, E., 1997. Role of delivery vehicles for photosensitisers in the photodynamic therapy of tumors. J. Photochem. Photobiol. B: Biol. 37, 189–195.

Ribó, J.M., Crusats, J., Farrera, J.A., Valero, M.L., 1994. Aggregation in water solutions of tetrasodium diprotonated meso-tetrakis(4-sulfonatophenyl)porphyrin. J. Chem. Soc., Chem. Commun., 681–682.

Ricchelli, F., 1995. Photophysical properties of porphyrins in biological membranes. J. Photochem. Photobiol., B: Biol. 29, 109–118.

Ricchelli, F., Gobbo, S., Moreno, G., Salet, C., Brancaleon, L., Mazzini, A., 1998. Photophysical propreties of porphyrin planar aggregates in liposomes. Eur. J. Biochem. 253, 760–765.

Ricchelli, F., Stevanin, D., Jori, G., 1988. Porphyrin-liposome interactions: influence of the physico-chemical properties of the phospholipid bilayer. Photochem. Photobiol. 48, 13–18.

Rouser, G., Fleischer, S., Yamamoto, A., 1970. Quantitative analysis of phospholipids by thin layer chromatography and phosphorus analysis of spots. Lipids 5, 494–496.

Sandberg, S., Romslo, I., 1981. Porphyrin-induced photodamage at the cellular and the subcellular level as related to the solubility of the porphyrin. Clin. Chim. Acta 109, 193–201.

Schieweck, K., Capraro, H.G., Isele, U., van Hoogevest, P., Ochsner, M., Maurer, T., Batt, E., 1994. Liposome-delivered zinc(II) phthalocyanine as a phototherapeutic agent for tumours. In: Jori, G., Moan, J., Star, W.M. (Eds.), Photodynamic Therapy of Cancer, Proceedings of SPIE Series, vol. 2078. SPIE, Bellingham, Washington, pp. 117–118.

Segalla, A., Milanesi, C., Jori, G., Capraro, H.G., Isele, U., Schieweck, K., 1994. A liposomal Ge(IV) Phthalocyanine bearing two axially ligated cholesterol moieties: a new potential agent for photodynamic therapy of tumours. Br. J. Cancer 68, 817–825.

Spikes, J.D., 1992. Quantum yields and kinetics of the photobleaching of hematoporphyrin, photofrin II, tetra(4-sulfonatophenyl)-porphine and uroporphyrin. Photochem. Photobiol. 55, 797–808.

Tanielian, C., Wolff, C., 1995. Porphyrin-sensitized generation, of singlet molecular oxygen: comparison of steady state and time-resolved methods. J. Phys. Chem. 99, 9825–9830.

Terazima, M., Hirota, N., Shinohara, H., Saito, Y., 1991. Photothermal investigation of the triplet state of C_{60}. J. Phys. Chem. 95, 9080–9085.

Venediktov, E.A., Krasnovsky Jr., A.A., 1982. Efficiency of luminescence generation of singlet molecular oxygen by porphyrins. Zh. Prikl. Spektrosk. 36, 152–154.

Verlhac, J.B., Gaudemer, A., Kraljic', I., 1984. Water-soluble porphyrins and metalloporphyrins as photosensitizers in aerated aqueous solutions. 1. Detection and determination of quantum yield of formation of singlet oxygen. Nouv. J. Chim. 8, 401–406.

Verma, A., Facchina, S.L., Hirsch, D.J., Song, S.-Y., Dillahey, L.F., Williams, J.R., Snyder, S.H., 1998. Photodynamic tumor therapy: mitochondrial benzodiazepine receptors as a therapeutic target. Mol. Med. 4, 40–45.

Zenkevich, E., Sagun, E., Knyukshto, V., Shulga, A., Mironov, A., Efremova, O., Bonnett, R., Songca, S.P., Kassem, M., 1996. Photophysical and photochemical properties of potential porphyrin and chlorin photosensitizers for PDT. J. Photochem. Photobiol. B Biol. 33, 171–180.